International Journal of Pharmaceutics 584 (2020) 119437

Contents lists available at ScienceDirect

International Journal of Pharmaceutics

journal homepage: www.elsevier.com/locate/ijpharm

Antimicrobial peptide Temporin-L complexed with anionic cyclodextrins results in a potent and safe agent against sessile bacteria

Diego Brancaccio[a], Elio Pizzo[b], Valeria Cafaro[b], Eugenio Notomista[b], Federica De Lise[b], Andrea Bosso[b], Rosa Gaglione[c], Francesco Merlino[a], Ettore Novellino[a], Francesca Ungaro[a], Paolo Grieco[a], Milo Malanga[d], Fabiana Quaglia[a], Agnese Miro[a,*], Alfonso Carotenuto[a,*]

[a] Department of Pharmacy, University of Naples Federico II, via D. Montesano 49, 80131 Naples, Italy
[b] Department of Biology, University of Naples Federico II, Naples, Italy
[c] Department of Chemical Sciences, University of Naples Federico II, Naples, Italy
[d] Cyclolab Cyclodextrin R&D Laboratory Ltd., H-1097 Illatos St. 7., Budapest, Hungary

ARTICLE INFO

Keywords:
Antibiotic resistance
Antimicrobial peptides
Cyclodextrins
Antibiofilm agents

ABSTRACT

Concern over antibiotic resistance is growing, and new classes of antibiotics, particularly against Gram-negative bacteria, are needed. Antimicrobial peptides (AMPs) have been proposed as a new class of clinically useful antimicrobials. Special attention has been devoted to frog-skin temporins. In particular, temporin L (TL) is strongly active against Gram-positive, Gram-negative bacteria and yeast strains. With the aim of overcoming some of the main drawbacks preventing the widespread clinical use of this peptide, i.e. toxicity and unfavorable pharmacokinetics profile, we designed new formulations combining TL with different types of cyclodextrins (CDs). TL was associated to a panel of neutral or negatively charged, monomeric and polymeric CDs. The impact of CDs association on TL solubility, as well as the transport through bacterial alginates was assessed. The biocompatibility on human cells together with the antimicrobial and antibiofilm properties of TL/CD systems was explored.

1. Introduction

The decreasing efficacy of conventional antibiotics in treating common infections has quickened in recent years, and with the arrival of untreatable strains of carbapenem-resistant *Enterobacteriaceae*, we are today in a post-antibiotic era (Jacob et al., 2013). The continued high rates of antibiotic use in hospitals, in the community and in agriculture have contributed to selection pressure that has sustained resistant strains, forcing a shift to more expensive and more broad-spectrum antibiotics. This misuse and overuse of antibiotics has led to antibiotic resistance among bacteria, consequent treatment complications and increased healthcare costs. Nowadays, there are many infections that are not adequately treated with conventional antibacterial drugs, such as lung/cutaneous and systemic infections due, for example, to the Gram-negative bacteria *Pseudomonas aeruginosa* and *Acinetobacter baumannii* (Woodford et al., 2014). For this reason, there is the need and urgency to overcome this trouble.

In this context, antimicrobial peptides (AMPs) are fascinating targets as novel antibiotics because of their broad-spectrum activity, which includes multidrug resistant (MDR) bacteria (Mookherjee and Hancock, 2007). AMPs are constitutive or inducible defense barriers against microbial infections in all living organisms, including humans. This class of agents is currently considered one of the most promising in fighting the emergence of bacteria resistant to conventional antibiotics. It is widely accepted that the main target of AMPs is the lipid bilayer of the bacterial membrane (Brogden, 2005). A large number of AMPs modulate the immune response or have targets within the cell, while others have multiple targets. Taking these findings together, AMPs display robust mechanisms that could decrease the possibility for resistance to develop requiring multiple alterations in different targets (Brogden, 2005). Nowadays, AMPs have a recognized potential for generating new drugs to increase the therapeutic tools effective against MDR and/or biofilm producing pathogens, especially useful for topical application and mucosal infections. It is worth noting, however, that several issues have hampered the development of AMP-based drugs so far. For instance, the lack of selectivity of natural antimicrobial peptides for bacteria often results in a certain degree of toxicity for eukaryotic cells. Furthermore, the way to the target is complicated by the biofilm-

* Corresponding authors.
E-mail addresses: agnese.miro@unina.it (A. Miro), alfonso.carotenuto@unina.it (A. Carotenuto).

https://doi.org/10.1016/j.ijpharm.2020.119437
Received 18 December 2019; Received in revised form 11 May 2020; Accepted 13 May 2020
Available online 21 May 2020
0378-5173/

like mode of growth that several bacteria adopt (Römling and Balsalobre, 2012) and by the slow transport through mucus which covers some regions where chronic infections occur (Cornick et al., 2015).

Among AMPs of natural origin, the amphibian temporins represent one of the largest families (more than 100 members) and are among the smallest-sized AMPs (10–14 amino acids) found in nature to date (Simmaco et al., 1996). In general, temporins are known to be highly active against Gram-positive bacteria. The only exception is represented by the isoform temporin L (TL, H-Phe^{1}-Val^{2}-Gln^{3}-Trp^{4}-Phe^{5}-Ser^{6}-Lys^{7}-Phe^{8}-Leu^{9}-Gly^{10}-Arg^{11}-Ile^{12}-Leu^{13}-NH_2) as it is strongly active also against Gram-negative bacteria and yeast strains (Rinaldi et al., 2002). Previously, our group has extensively studied the mechanism of action and developed novel analogs of this interesting AMP (Buommino et al., 2019; Grieco et al., 2013, 2011; Merlino et al., 2017). Nevertheless, TL self-aggregation is responsible for low solubility and impaired bioactivity (Mahalka and Kinnunen, 2009), which severely hampers its translation into clinical use.

Cyclodextrins (CDs) are starch-derived cyclic sugars capable of including a variety of hydrophobic guests and comprise a large family of native and semisynthetic derivatives, some of which being already approved in medicinal products (Miro et al., 2011). Due to the presence of a hydrophobic cavity, CDs can interact with lipophilic groups fitting size requirement for host–guest complexation, thus improving guest apparent solubility in aqueous media (Uekama et al., 2006). Beside small hydrophobic molecules, CDs can interact with peptides/proteins through the hydrophobically-driven binding of aromatic amino acids (tyrosine, tryptophan, phenylalanine, histidine) (Challa et al., 2005; Pandey et al., 2010). By including these lipophilic moieties, CDs can decrease the flexibility of peptides because of the formation of a hydrogen-bond network (Yeguas et al., 2011).

In this work, we aimed at developing novel TL formulations endowed with improved activity toward bacterial target. To this purpose, TL was associated to a panel of neutral or negatively charged, monomeric and polymeric CDs which are expected to interact with the peptide through both hydrophobic and electrostatic interactions, possibly limiting its self-aggregation. The impact of CDs association on TL solubility, their interaction mode, as well as the transport through bacterial alginates was assessed and the antimicrobial and antibiofilm activities of TL/CD systems, respectively against a panel of planktonic bacterial strains and sessile methicillin-resistant *Staphylococcus aureus* (*MRSA*) and *wild-type P. aeruginosa* (*PAO1*), were explored.

2. Materials and methods

2.1. Materials

Temporin L (TL, MW = 1981 Da) was achieved according to the ultrasound-assisted solid-phase peptide synthetic (US-SPPS) strategy, elsewhere reported (Merlino et al., 2019) Hydroxypropyl-β-cyclodextrin (HPβCD Pharma Grade), carboxymethyl-β-cyclodextrin sodium salt (CMβCD fine chemical grade) and sulfobutylated-β-cyclodextrin sodium salt (pharma grade) were from CycloLab. Poly(β-cyclodextrin) (pβCD, fine chemical grade), Poly(carboxymethyl-β-cyclodextrin) (pCMβCD, fine chemical grade) were synthesized as previously described (Malanga et al., 2014). All the fine chemical grade cyclodextrin products were extensively dialyzed on a Spectra/Por™ Dialysis Membrane Tubing (cut-off 100–500 Da) before lyophilization. Epichlorohydrin (99%), sodium hydroxide (85%), 1.4-butane sultone (99%) were purchased from Sigma-Aldrich; β-CD was obtained from Wacker Chemie (Germany). Capillary electrophoresis (CE) experiments were conducted on an Agilent 7100 Capillary Electrophoresis System equipped with Diode Array Detector (Waldbronn, Germany). Molecular weight determination was performed using a Malvern Zetasizer Nano ZS instrument running a Static Light Scattering (SLS) method. Ultrapure water was employed throughout the study.

2.2. Synthesis of Poly(sulfobutylated-β-cyclodextrin)

In order to introduce the sulfobutyl moieities mainly, but not exclusively, on the cyclodextrin units, the alkylation step (sulfobutylation) was performed according to a one-pot pre-branching functionalization (Supplementary material, Fig. S1). In particular, native βCD (10 g, 8.8 mmol) was dissolved in water (32 mL), NaOH (1.26 g, 31.2 mmol) was added and the reaction mixture was heated to 60 °C and stirred for 10 min. 1,4-butane sulfone was dropwise added to the pre-heated solution within 30 min. The reaction mixture was stirred for additional 90 min at 60 °C and for 12 h at room temperature. A second portion of NaOH (2.5 g, 62.5 mmol) was added and stirred for 10 min then epichlorohydrin (4.8 mL, 60 mmol) was added and the reaction mixture was heated at 70 °C for 3 h. The solution was cooled down to room temperature, neutralized with aqueous HCl solution (5 M) and dialyzed against deionized water for 48 h. Freeze-drying yielded the titled compound as white powder.

CD content based on ^{1}H NMR: 58% (w/w). Degree of substitution (DS) for sulfobutyl based on ^{1}H NMR: 2.5. 4-Hydroxybutane-1-sulfonic acid residual level based on CE: 0.09%. Bis(4-sulfobutyl)ether disodium residual level based on CE: 0.05%. Molecular weight based on static light scattering: 80 ± 13 kDa. CD properties are reported in Table S1 (Supplementary material).

2.3. TL/CDs complexation

A 2.5 mM stock TL solution was prepared in water (5 mg mL^{-1}). To allow TL complexation with the different CDs, 40 μL of this stock solution was added to 40 μL of a water solution containing monomeric CDs (TL/CDs 1:1 M ratio) or polymeric CDs (500 μg) and diluted to a total of 800 μL with water to achieve a 0.125 mM TL solution. Samples were frozen at −25 °C and freeze-dried at 0.01 atm for 24 h.

2.4. Spectroscopic characterization of TL/CDs

TL/CDs aqueous solutions ([TL] = 0.125 mM) and freeze-dried powders reconstituted in 800 μL of phosphate buffer saline (PBS) at pH 7.4 (7 g of sodium chloride, 0.2 g potassium chloride and 1.8 g disodium hydrogen phosphate *per liter*) to achieve the same TL concentration, were analyzed by UV–vis/fluorescence and NMR spectroscopy. UV–vis spectra were collected on a UV-1800 (Shimadzu) (1 cm quartz cell length) while fluorescence excitation/emission spectra were collected on a RF-6000 spectrofluorimeter (Shimadzu).

2.5. NMR spectroscopy

NMR spectra were recorded on a Varian INOVA 700 MHz spectrometer equipped with a z-gradient 5 mm triple-resonance probe head. All the spectra were recorded at a temperature of 25 °C. One-dimensional (1D) NMR spectra were recorded in the Fourier mode with quadrature detection. The water signal was suppressed by gradient echo (Hwang and Shaka, 1995). Two dimensional (2D) TOCSY (Braunschweiler and Ernst, 1983), and NOESY (Jeener et al., 1979) spectra were recorded in the phase-sensitive mode using the method from States (States et al., 1982). Data block sizes were 2048 addresses in t_2 and 512 equidistant t_1 values. Before Fourier transformation, the time domain data matrices were multiplied by shifted $\sin^2$ functions in both dimensions. A mixing time of 70 ms was used for the TOCSY experiments. NOESY experiments were run with mixing times in the range of 200–300 ms. Complete ^{1}H NMR chemical shift assignments were effectively achieved for all the analyzed peptides according to the Wüthrich procedure (Supplementary material, Table S2) (Wüthrich, 1986).

2.6. Docking procedure

Initial β-cyclodextrin structure from pdb (3CGT) was modified using the Builder module of InsightII (Accelrys, San Diego, CA) to obtain the CMβCD. Considering the mean degree of substitution (Table S1), four carboxymethyl groups were added to the βCD; one on the primary and three on the secondary OH-face (the last linked to the hydroxyl groups in position 2), according to NMR analysis (data not shown). Exact carboxymethyl positions were randomly chosen. CMβCD was energetically minimized using the steepest descent method for 10,000 steps. NMR structure previously obtained by us (Carotenuto et al., 2008) was used as TL initial structure. Docking study was accomplished using the program DINC 2.0 (Antunes et al., 2017; Dhanik et al., 2013). The docking area was centered on the cyclodextrin center of mass. A set of grids of 60 Å x 60 Å x 60 Å was calculated around the docking area for the ligand atom types. Refinement of lowest energy pose of TL/CMβCD complex was achieved by in vacuo energy minimization with the Discover algorithm (Accelrys) using the steepest descent and conjugate gradient methods until a RMSD of 0.05 kcal/mol per Å was reached. After minimization the interaction energies were −49.4 (Van der Waals energy) and −748.7 kcal/mol (electrostatic energy).

2.7. Permeation of TL through bacterial alginates

The penetration of TL and TL/CDs through bacterial alginates was investigated through a diffusion experiment model previously developed (D'Angelo et al., 2015). Briefly, 75 μL of bacterial alginates (Alginate/Nonacetylated polymannuronic acid 1%/1% by wt (average Mw greater than 5000 Da) Carbosynth, U.K.) were placed in the upper chambers of Transwell® −12 well plates (12 mm diameter, polyester membranes with 3.0 μm pore size), whereas 300 μL of water were added in the lower chamber. At scheduled time intervals (from 0 to 24 h), the receptor medium was collected and analyzed for TL content at Ex/Em = 280/348 nm as reported above. The linearity of the response was analyzed at the concentration range 0.1–12.5 μg/mL ($r^2 \geq 0.999$).

2.8. Antimicrobial activity

Antimicrobial activity of TL, CDs and TL/CDs complexes was tested against *MRSA* WKZ-2, *Bacillus globigii* TNO BMO13, wild-type *P. aeruginosa* PAO1 and *Salmonella enterica* subsp. *enterica serovar Typhimurium* ATCC 14,028 as previously described (Bosso et al., 2017). Briefly, bacteria were grown to mid-logarithmic phase in Luria Bertani broth (LB) at 37 °C. Cells were then diluted to 1×10^6 CFU/mL in Difco 0.5X Nutrient Broth (Becton-Dickenson, Franklin Lakes, NJ) containing increasing amounts of TL, CDs, and TL (0,49–31,2 μM) complexed with CDs. Starting from a peptide stock solution, two-fold serial dilutions were sequentially carried out, accordingly to broth microdilution method (Wiegand et al., 2008). Following over-night incubation, MIC_{100} values were determined as the lowest peptide concentration responsible for no visible bacterial growth.

2.9. Eukaryotic cell culture and cell viability MTT assay

Human keratinocytes (HaCaT) cell line were cultured in high-glucose Dulbecco's modified Eagle's medium (DMEM) supplemented with 10% FBS, 1% Pen/strep at 37 °C and 5% carbon dioxide (CO_2). MTT cell viability assay was performed after seeding HaCaT cells on 96-well plates at a density of 4×10^3 cells/well in 0.1 mL of complete DMEM 24 h prior to the treatment. Cells were incubated in the presence of different samples at a final concentration of 7.5, 15 and 30 μM, for 36 h. As control, cells were incubated with PBS 1X buffer diluted in medium. Cell viability was evaluated by MTT assay, adding tetrazolium MTT (3-(4,5-dimethylthiazol-2-yl)-2,5-diphenyltetrazolium bromide) diluted at 0.5 mg/mL in DMEM without red phenol (0.1 mL/well). After 4 h of incubation at 37 °C, the resulting insoluble formazan salts were solubilized in 0.04 M HCl in anhydrous isopropanol and quantified by measuring the absorbance at λ = 570 nm, using an automatic plate reader spectrophotometer (Synergy ™ H4 Hybrid Microplate Reader, BioTek Instruments, Inc., Winooski, Vermont, USA). Cell survival was expressed as means of the percentage values compared to control. Data derived from at least three independent experiments.

2.10. Microtiter plate biofilm assay

Biofilm formation was analyzed by using a static abiotic solid surface assay, as previously described (Gaglione et al., 2017). To this purpose, stationary phase *wild-type P. aeruginosa* PAO1 and *MRSA* WKZ-2 cells, obtained from an *over-night* culture, were diluted 1/100 in 0.5X MHB. Assays were carried out in sterile 96-well polypropylene microtiter plates (Costar Corp., Cambridge, MA) in presence of different concentrations of either TL or TL/CDs complex. Bacteria in absence of compounds were used as a positive control, whereas buffer in absence of bacteria was used as a negative control. Incubations were carried out for 4 h, in order to test compounds effects on biofilm attachment, and on preformed biofilm, in order to test their effects on biofilm detachment. When the effects on preformed biofilm were evaluated, bacterial biofilms were formed for 24 h at 37 °C, and then treated with increasing concentrations (0–4 μM) of molecules under test. In all cases, at the end of the incubations, the crystal violet assay was performed. Samples were gently washed with PBS 1X, in order to remove planktonic cells, whereas biofilm biomass was stained with 0.1% crystal violet (Sigma Aldrich, Milan, Italy). Biofilm stained biomass was transferred into flat-bottom polystyrene 96-well plate and optical densities at 595 nm were measured using a microtiter plate reader (Synergy ™ H4 Hybrid Microplate Reader, BioTek Instruments, Inc., Winooski, Vermont, USA).

2.11. Confocal microscopy (CLSM) analysis of static biofilm growth

Bacterial biofilm was grown on glass cover slips in 24-well plates in 0.5X MHB in static conditions. In particular, bacterial cells from an *over-night* culture were diluted to about $1x10^8$ CFU/mL and then seeded into wells for 24 h at 37 °C. Afterwards, non-adherent bacteria were removed by gently washing samples with sterile phosphate buffer and incubations with TL or TL/CDs ([TL] = 0.25 μM) were performed for further 24 h to evaluate their ability to eradicate the preformed biofilm.

Glass cover slips were then mounted in phosphate buffer. Viability of cells embedded into biofilm structure was determined by sample staining with LIVE/DEAD® BacLight™ Bacterial Viability kit (Molecular Probes Thermo Fisher Scientific, Waltham, MA, USA). Staining was performed accordingly to manufacturer instructions. Biofilm images were captured by using a confocal laser scanning microscopy (Zeiss LSM 710, Zeiss, Germany) and a 63X objective oil immersion system. Biofilm architecture was analyzed by using the Zen Lite 2.3 software package. Each experiment was performed in triplicate. All images were taken under identical conditions.

2.12. Statistical analysis

Results are presented as the mean ± standard error of the mean (SEM) of at least three independent experiments. Statistical significance was assessed using Student's t-Test. All samples were compared to the negative control and to the TL alone; significant differences were indicated as *($P < 0.05$), **($P < 0.01$) or ***($P < 0.001$) and are reported in the Supplementary material (Tables S3-S5).

3. Results

3.1. Spectroscopic and solubility features of TL

TL is a cationic peptide (+2 positive charges) containing aromatic

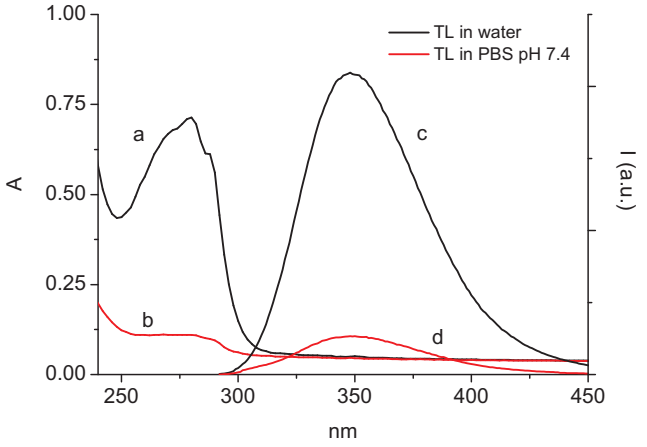

Fig. 1. UV–vis absorption and fluorescence emission spectra (λ_{ex} = 280 nm) of TL in water at pH 5 (a, c) and PBS at pH 7.4 (b, d). [TL] = 0.1 mM.

and positively-charged amino acids which are ionized at physiological pH. As shown in Fig. 1, TL in water at pH 5 (due to the presence of trifluoroacetic acid) shows a maximum absorption at 280 nm, which is typical of aromatic rings, and a fluorescence emission at 350 nm due to the presence of a tryptophan residue in the amino acid sequence. UV–vis absorption and fluorescence emission are depressed when TL is dissolved in PBS at pH 7.4, highlighting its prospective poor solubility in biological fluids.

Since primary sequence of TL contains both aromatic and positively charged amino acids, a library of neutral and anionic monomeric and polymeric β-cyclodextrin derivatives was selected in view of their possible interactions with TL through both hydrophobic and electrostatic interactions. To better explore the impact of anionic charge, also a novel negatively-charged polymeric sulfobutyl ether β-cyclodextrin was synthesized *ad hoc* (Fig. S1). The structure and properties of the CDs selected for this study are reported in Fig. S2 and Table S1, respectively.

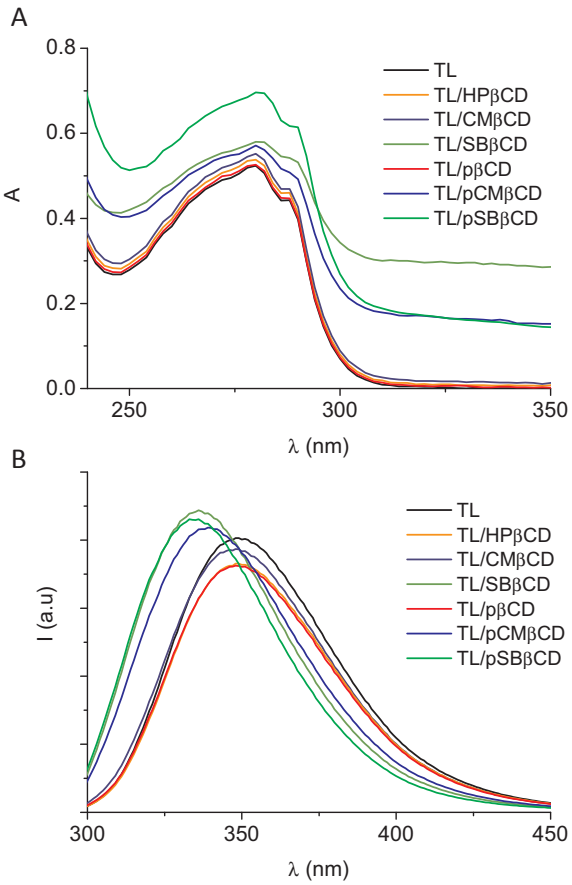

Fig. 2. (A) UV absorption spectra and (B) fluorescence emission spectra (λ_{ex} = 280 nm) of TL/CDs aqueous solutions ([TL] = 0.125 mM). For the UV spectra, baseline correction with each CDs aqueous solutions at the same concentration that was used in the complex was carried out. The color code for each TL/CD system reported here will be used throughout the text.

3.2. Interaction of TL and CD derivatives

UV–vis spectra of TL and TL/CDs samples/systems in water at pH 5, where TL displays the highest solubility, are shown in Fig. 2A. Baseline correction of absorption spectra with CDs solutions was needed since polymeric CDs showed an absorption band with maximum centered at 264 nm.

To set comparable conditions for all the tested CDs, baseline correction was applied also in the case of monomeric CDs although they did not show any significant UV absorption. Spectra highlight a relevant scattering of solutions when SBβCD, pSBβCD and pCMβCD are employed, which is not attenuated when CDs aqueous solutions at the same concentration are used for baseline correction (cfr with spectra collected using water as baseline, Supplementary material Fig. S3). This effect suggests that these CDs derivatives can form aggregates with positively-charged TL. Emission spectra of the same samples (Fig. 2B) show an hypsochromic effect and a slight increase of fluorescence intensity at maximum wavelength in the samples with SBβCD, pSBβCD and pCMβCD, while there is no relevant effect for the other derivatives. Nevertheless, excitation spectra collected at λ_{em} = 350 nm give an absorption at TL absorption maximum, confirming that the fluorescence emission is due to tryptophan residue of TL (Supplementary material, Fig. S4).

^{1}H NMR data in deuterated aqueous solution confirmed that interactions between TL and anionic cyclodextrin derivatives occurred, since the peptide signals clearly changed in the presence of these CDs (Fig. 3). In particular, proton signals of the TL/HPβCD system are almost unchanged while they show only some broadening with pβCD but without any significant chemical shift changes. In contrast, many TL signal chemical shifts varied upon CMβCD addition and all of them almost disappeared upon interaction with pCMβCD, SBβCD, and pSBβCD. This signal disappearance demonstrates the formation of high molecular weight complexes where ^{1}H NMR signals broaden due to the reduction of the transverse relaxation time (T_2). In the case of TL/SBβCD complex, the broadening ascertains the formation of molecular aggregates at the investigated concentration (0.125 mM) since the MW of the soluble complex is expected to give detectable ^{1}H NMR signals.

The complex TL/CMβCD was further investigated by NMR because, as mentioned above, the TL signals shifted due to the interaction with the CMβCD but, at the same time, they remained visible and thus available for in-depth studies. 2D TOCSY and NOESY spectra allowed complete signal assignment of the peptide (Table S2), which allowed to find out that the resonances of protons belonging to Phe^1, Gln^3, and Trp^4 are the most influenced by complex formation (Supplementary material, Fig. S5). Unfortunately, no intermolecular NOEs could be observed in the NOESY spectrum of the complex, which prevented further interaction details from being obtained.

A molecular model of the complex was obtained by automatic docking procedure (DINC 2.0) which evidenced that the complex is stabilized mainly by electrostatic interactions and confirmed that the N-terminal region of TL is the most affected by the CMβCD interaction (Fig. 4). In this model, Trp^4 indole forms hydrophobic interactions with the cavity of CD, the indole NH proton of the same residue forms a hydrogen bond with a sugar hydroxyl group, Gln^3 side chain amide protons form a hydrogen bond with a carboxyl group of the CMβCD,

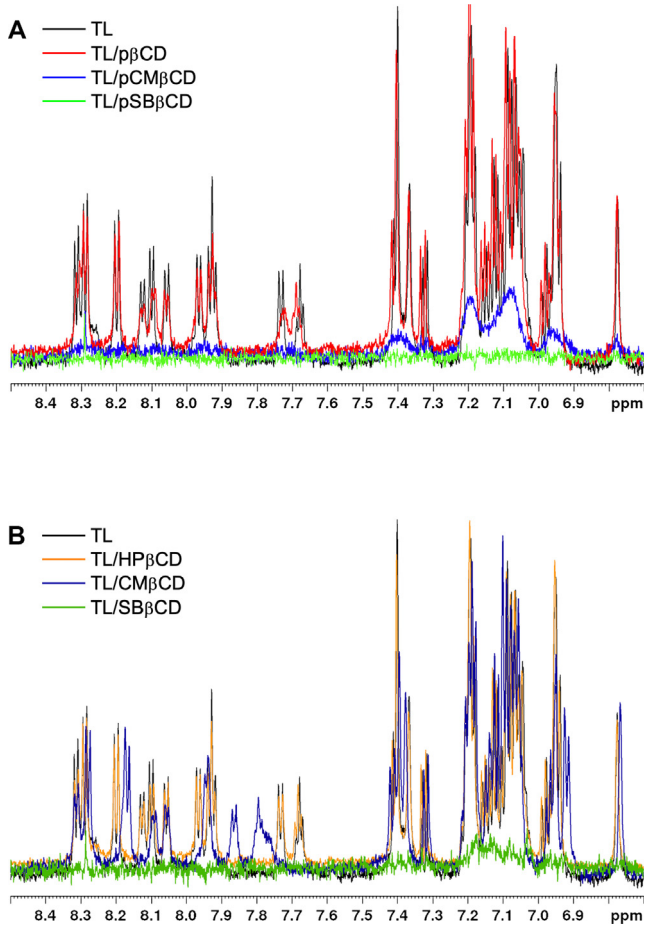

Fig. 3. Low-field region of the ^{1}H NMR spectrum of TL in complex with polymeric (A) or monomeric (B) CDs in deuterated aqueous solution. TL is always reported for comparison.

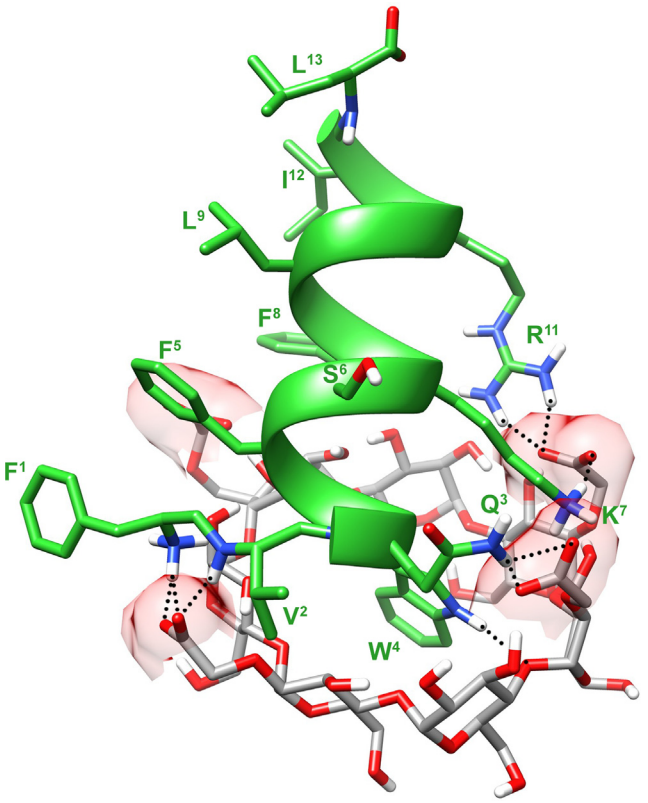

Fig. 4. Molecular model of TL/CMβCD complex. Peptide backbone is reported as green ribbon. Oxygen and nitrogen atoms are reported in red and blue, respectively. Carbon atoms are reported in green for TL and grey for CMβCD. Non polar hydrogen atoms are not shown for clarity. CMβCD carboxyl groups are evidenced as pink surface. Hydrogen bonds are evidenced as dotted lines. (For interpretation of the references to color in this figure legend, the reader is referred to the web version of this article.)

and the terminal amine, Lys^{7}, Arg^{11} groups form charged reinforced hydrogen bonds with other carboxyl groups of the CMβCD.

3.3. Solubility of TL/CD derivatives in physiological conditions

TL/CDs aqueous solutions were freeze-dried and the pellet redispersed in physiological conditions (PBS, pH 7.4). UV–vis spectra of the reconstituted TL/CD samples (same amount of TL) at 0.125 mM (Supplementary material, Fig. S6) were not informative on a putative solubilization enhancement exerted by CDs. On the contrary, fluorescence emission spectra (Fig. 5A) highlighted how polymeric derivatives increased fluorescence emission, which can be reasonably attributed to an increased amount of TL in the medium. It is worth noting that the highest blue-shift observed occurs for anionic pCDs confirming that Trp insertion in the CD cavity is assisted by the presence of positive groups in TL.

By comparing the integral of fluorescence spectra intensity of TL/CDs samples with that of TL in water (Supplementary material, Fig. S7), a solubility enhancement factor was calculated (Fig. 5B). Data demonstrate that all the CD polymers are much more efficient in allowing an increase of TL amount dissolved in PBS as compared to corresponding monomeric CDs. The slow increase of TL solubility for monomeric CDs can be roughly attributable to the freeze-drying effect procedure (cfr with enhancement factor for TL alone after freeze-drying) which likely results in sample amorphization and more efficient solubilization.

The total amount of TL in PBS has to be attributed to both TL readily solubilized and TL aggregates redispersion. In fact, ^{1}H NMR data in PBS were generally similar to those obtained in water (Supplementary material, Fig. S8). Proton signals of TL in the presence of neutral cyclodextrin HPβCD and pβCD were virtually unchanged, while they nearly disappeared with polymeric negatively charged pCMβCD and pSBβCD. Differently from the aqueous solution, TL chemical shifts showed only minor variations upon CMβCD addition, and monomeric SBβCD did not cause TL signals disappearance but only their broadening and shift modification, mainly for aromatic signals. Hence, negatively charged CMβCD and SBβCD monomers seem to interact to a lesser extend with TL in PBS as compared to the aqueous solution.

3.4. Transport of TL through bacterial alginates

TL capability to cross a gel barrier as a surrogate of bacterial biofilm was investigated through a transport experiment illustrated in Fig. 6. The experiment consists in following the amount of TL permeated through a layer of bacterial alginates from a donor phase to an aqueous receptor phase and provides insight in the effect of complexation on TL mobility in the alginate gel. The amount of TL permeated for monomeric and polymeric CDs are reported in Fig. 6B and 6C, respectively. Overall, TL permeated after 24 h was slightly higher with HPβCD and roughly two-fold higher for pCMβCDs as compared to TL alone.

3.5. TL/CDs activity against planktonic bacteria

The antibacterial effectiveness of TL, CDs and TL/CDs systems on planktonic bacteria was determined by measuring minimum inhibitory concentration (MIC) on four bacterial strains: two Gram-negative (*wild-type P. aeruginosa* PA01 and *Salmonella enterica* subsp. *enterica serovar*

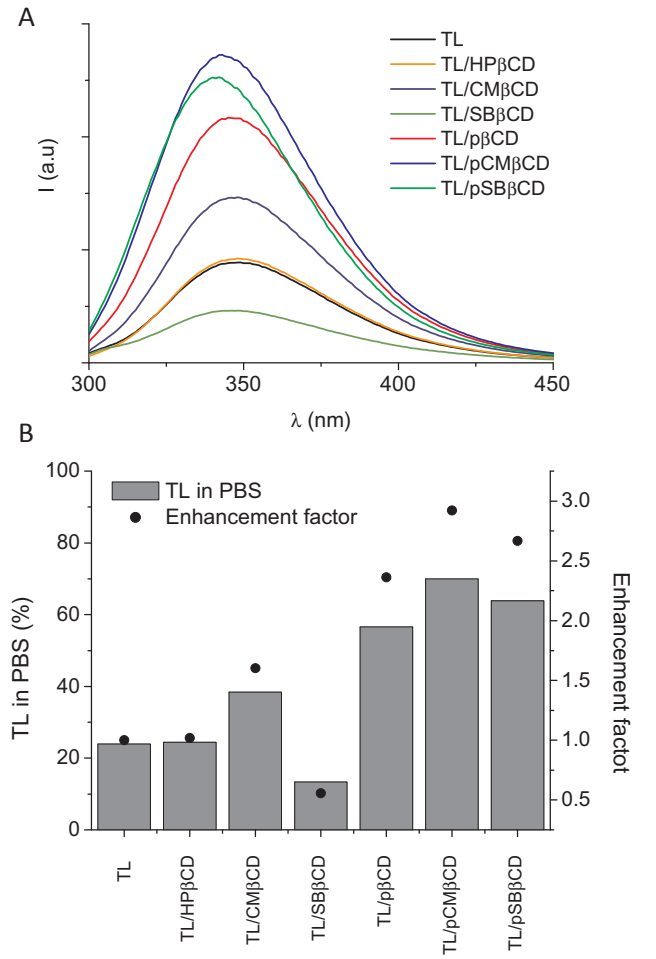

Fig. 5. A) Fluorescence emission spectra (λ_{ex} = 280 nm) of TL/CDs solutions in PBS at pH 7.4 ([TL] = 0.125). B) Amount of TL in PBS and solubility enhancement factor due to the presence of CD. Enhancement factor is the ratio between the integral of fluorescence emission spectra collected for each TL/CDs system and freeze-dried TL.

Typhimurium ATCC 14028) and two Gram-positive (*MRSA* WKZ-2 and *Bacillus globigii* TNO BMO13) strains (Table 1). As already mentioned, TL is the only temporin active on Gram-negative as it also emerges from the MIC carried out on *P. aeruginosa* PA01 and *Salmonella enterica* ATCC 14028. As reported in Table 1, TL/CDs systems generally preserve the antimicrobial activity of the free peptide and, to date, CDs at the same amount employed for TL complexation had no antimicrobial activity *per se* (data not shown).

3.6. Anti-Biofilm activity of TL and TL/βCDs

Since wild-type *P. aeruginosa* PAO1 and *methicillin resistant S. aureus* (*MRSA*) are strong biofilm producers, here we investigated the anti-biofilm properties of TL and TL/CDs against these clinical isolated bacteria. Crystal violet (CV) staining assays were performed to determine the percentage of attached and preformed biofilm in the absence or presence of increasing concentrations of each compound (Fig. 7). A significant reduction (see Tables S3-4 for statistical analysis) of the attached biofilm treated with 4 μM of TL or TL/CDs in the case of both Gram-positive *MRSA* (Fig. 7A) and Gram-negative *P. aeruginosa* (Fig. 7C) was found. The obtained results highlight that the complexes TL/CDs are more able to inhibit the biofilm attachment with respect to the TL alone in the case of TL/SBβCD, TL/HPβCD and TL/pβCD considering *MRSA* (Fig. 7A) and in the case of TL/HPβCD and TL/pβCD for *P. aeruginosa* (Fig. 7C). A reduction of biofilm mass was also observed

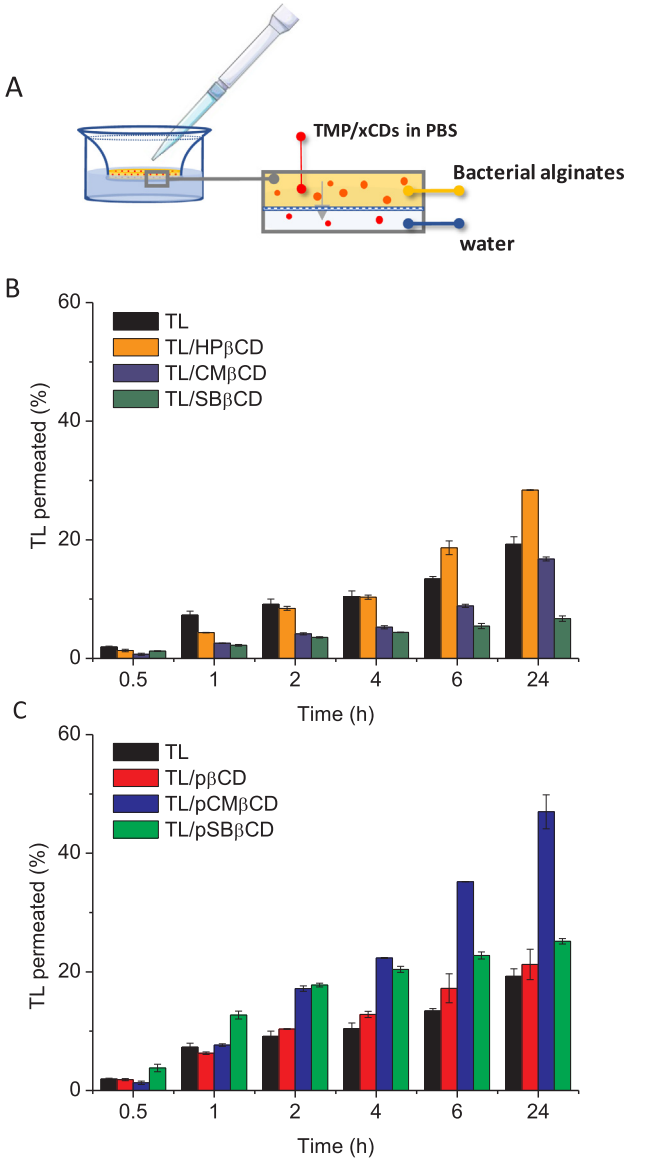

Fig. 6. A) Set-up of the transport experiment of TL through bacterial alginates. Amount of TL permeated in the receptor phase when TL in the donor phase is associated to B) monomeric CDs or C) polymeric CDs.

Table 1
Minimal inhibitory concentration (μM) of TL/CDs complexes on different strains of planktonic bacteria.

	Wild-type *PAO1*	*S. enterica* ATCC 14028	*MRSA* WKZ-2	*B. globigii* TNO-BMO13
TL	3.9	3.9	3.9	1.9
TL/HPβCD	7.8	3.9	3.9	F1.9
TL/pβCD	3.9	3.9	1.9	1.9
TL/SBβCD	15.6	1.9	15.6	0.95
TL/pSBβCD	3.9	7.8	3.9	3.9
TL/CMβCD	3.9	1.9	1.9	0.95
TL/pCMβCD	7.8	7.9	3.9	3.9

when pre-formed biofilms were treated at the lowest concentration (0.25 μM) of TL and TL/CDs with respect to the control, for both bacterial strains (Fig. 7B and D).

In order to further investigate the anti-biofilm properties of TL and TL/CDs, we also performed analyses by using confocal microscopy. We analyzed the effects of both TL or TL/βCDs at sub-MIC concentration

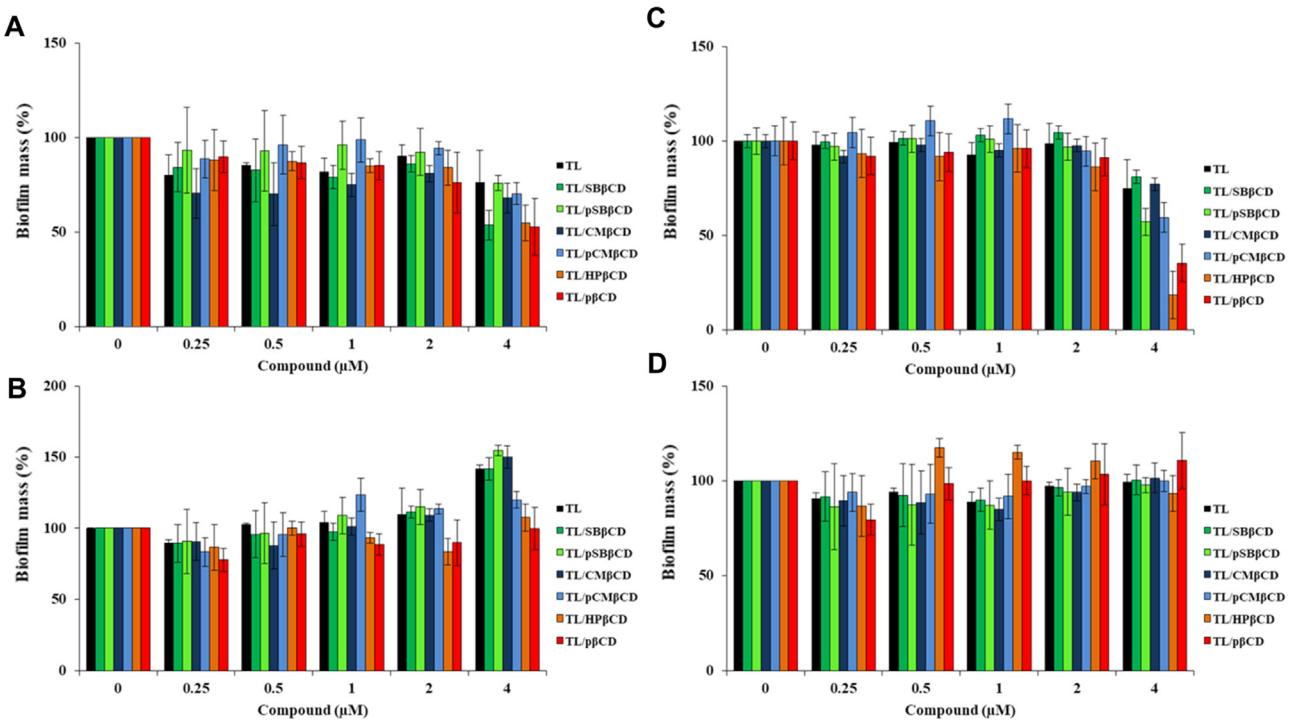

Fig. 7. Anti-biofilm activity of TL and TL/CDs on *MRSA* (A, B) and *P. aeruginosa* PAO1 (C, D). The effects of increasing concentrations of the compounds were evaluated either on biofilm attachment (A, C) or on preformed biofilm (B, D). Data represent the mean (± standard deviation, SD) of at least three independent experiments, each one carried out with triplicate determinations.

(0.25 μM) on *MRSA* and *P. aeruginosa* pre-formed biofilms. In particular, bacterial cells from an *over-night* culture were diluted to about $1x10^8$ CFU/mL and then seeded into wells for 24 h at 37 °C. Afterwards, incubations with each compound (0.25 μM) were performed for further 24 h to evaluate their ability to eradicate the preformed biofilm. Following incubation, chambers were double stained (Syto-9/PI mix), in order to discriminate between live and dead biofilm cells.

As shown in Fig. 8A and 9A-B, all compounds affected *MRSA* biofilm, with the strongest effect obtained in the case of TL/SBβCD and TL/HPβCD (see Table S5 for statistical analysis).

Indeed, the biofilm height of samples treated with these compounds was reduced of about 50% compared to untreated sample (Fig. 9B). Moreover, sample treated with each TL/CD displayed a significant decrease in fluorescence intensity with respect to TL-treated sample together with reduced cell cohesion, which may be indicative of a disrupted extracellular matrix (Figs. 8 and 9A).

In the case of PAO1, instead, the strongest effect on the biofilm eradication has been obtained under treatment with TL/SBβCD and TL/pSBβCD (Fig. 9C and D). The other TL/CDs were able to reduce preformed biofilm with respect to the control, even if their effects were comparable to TL alone. It has to be noted that no significant effects were found under TL/CMβCD treatment.

3.7. Cytotoxic effect

Biocompatibility of TL and TL/CDs systems was evaluated testing their effect on human keratinocytes (HaCaT) cell line performing an MTT assay as described in Materials and Methods. Following this method, cells were seeded on 96-well plates and treated with each sample at different concentrations (7.5, 15 and 30 μM) for 36 h. Cell survival was expressed as the ABS of blue formazan measured at 570 nm with an automatic plate reader. Three independent experiments were performed. Results shown in Fig. 10 underlined that TL alone is highly cytotoxic for HaCaT cells, in accordance with data reported in the literature (Grieco et al., 2013). Interestingly, 15 μM of TL/SBβCD, TL/pSBβCD, TL/CMβCD and TL/pCMβCD complexes showed significantly lower toxicity as compared with TL alone. Cyclodextrins (CDs) alone did not seem to be toxic for HaCaT cells (Supplementary material, Fig. S9).

4. Discussion

Nowadays, the use of antimicrobial peptides as therapeutic agents is one of the most attractive options to face the problem of antibiotic resistance due to numerous advantages such as their broad-spectrum activity, low toxicity and limited bacterial resistance observed in *vitro*. However, their use is limited because of the large amount of peptide required to exert the microbicidal function in *vivo* and due to the absence of a correct delivery platform. Additionally, solubility is a key issue for some peptides as in the case of TL which suffers from extensive aggregation due to formation of intermolecular bonds (Mahalka and Kinnunen, 2009).

In line with previous report (Mahalka and Kinnunen, 2009), TL exhibits excellent solubility in water, but very low solubility in PBS due to aggregation phenomena (Fig. 1), which could hamper its availability at the target microbe. In this context, association of TL with CD cavity could be useful to limit intramolecular bond formation in the peptide due to lipophilic amino acid side groups *via* establishment of novel interactions. Furthermore, electrostatic interactions between TL (positive charge, one lysine and one arginine in the primary structure with parallel absence of aspartic and glutamic acid residues) and anionic CDs could have an impact on TL self-aggregation but also on net charge of the host-guest complex. TL association with CDs was accomplished in aqueous environment to ensure full availability of TL groups and establishment of hydrophobic/electrostatic interactions with each CD derivative. Spectroscopic analysis of TL/CDs in water at pH 5 evidenced that TL interacts with anionic CD derivatives giving aggregation except for CMβCD as determined by scattering (Fig. 2) and solution NMR (Fig. 3). The observed blue-shift of TL emission spectra with pCD, and in a less extent with CMβCD, can be reasonably attributed to the non-

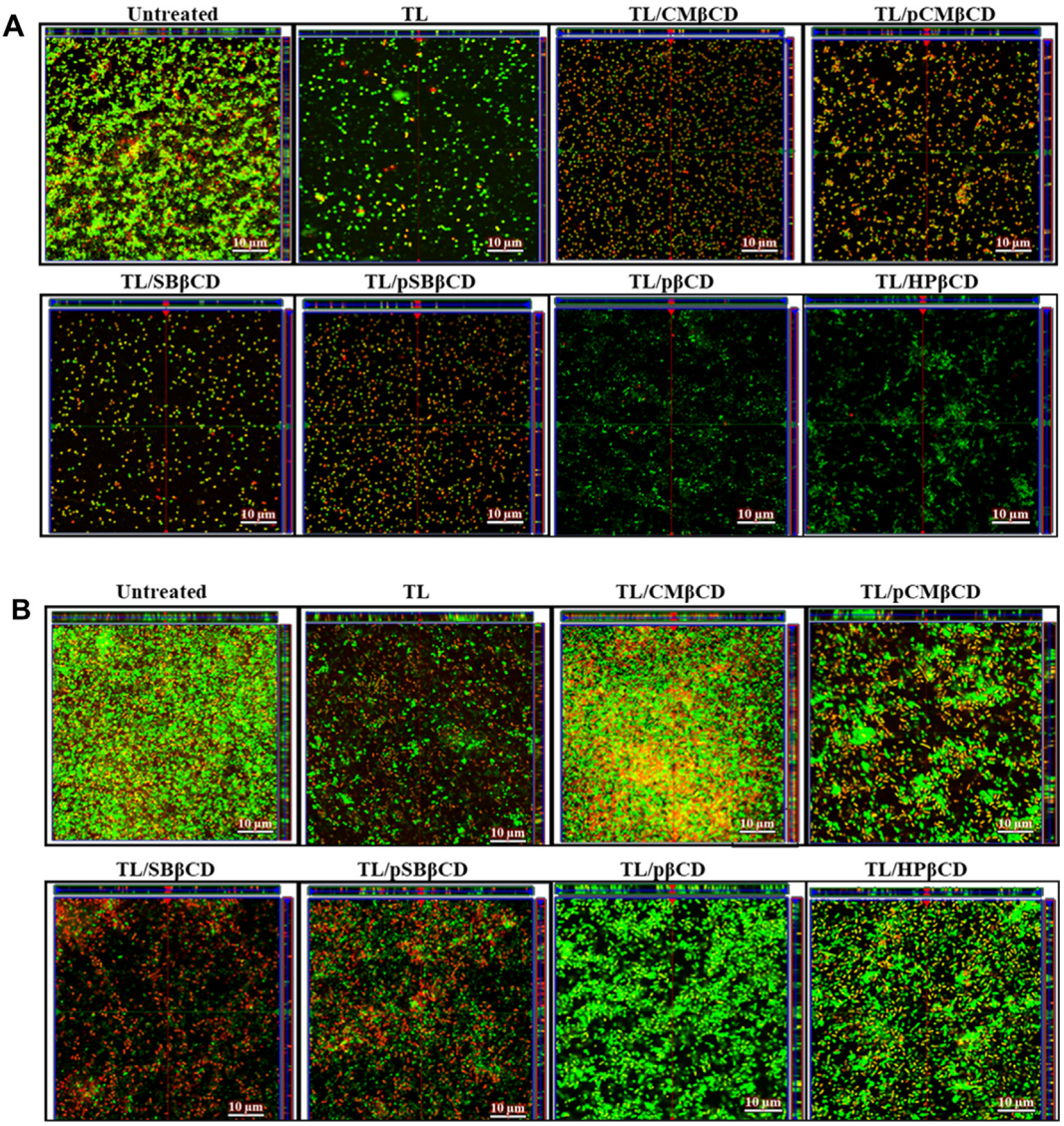

Fig. 8. Analysis of the effect of TL and TL/CDs on static biofilm growth by CLSM imaging. *MRSA* (A) and *P. aeruginosa* PAO1 (B) biofilm were grown for 24 h grown on glass cover slips in 24-well plates and then incubated in fresh MHB 0.5X, in the absence (control) or in the presence of TL and TL/CDs ([TL] = 0.25 μM). Biofilm cells were stained by using LIVE/DEAD BacLight bacterial viability kit (Molecular Probes, Eugene, OR) containing 1:1 ratio of Syto-9 (green fluorescence, all cells) and propidium iodide (PI; red fluorescence, dead cells). Images are 2D projections of biofilm structure obtained by confocal z-stack using Zen Lite 2.3 software. All images were taken under identical conditions. Scale bar corresponds to 10 μm in all the cases.

polar environment experienced by Trp (Teale, 1960), likely due to interaction with CD cavity which is amplified in the case of pCDs.

On the contrary, hydrophobic interactions between Trp of TL and CD cavity in neutral derivatives were not observed at all. Soluble TL/CMβCD complex was deeply investigated by 2D NMR and docking analyses. Both NMR (Fig. S5) and docking (Fig. 4) showed that the N-terminal region of TL is the most involved in the CMβCD interaction. Docking results evidenced that the complex is stabilized mainly by the electrostatic interactions. In particular, ionic bonds occur between the carboxyl groups on the primary CMβCD's face and peptide positively charged groups. Trp indole moiety is inserted in the hydrophobic cavity of the CMβCD in accordance with the slight blue shift of tryptophan fluorescence and the shift of the Trp ^{1}H NMR signals. Since, the weak acidic carboxylic groups are only partially deprotonated at the acidic pH in the samples prepared in water, the complex model shown in Fig. 4 is more representative of the status in physiological condition (pH 7.4). Accordingly, fluorescence emission spectra of the TL complexes with anionic pCDs in buffered solution (Fig. 5A) show again blue-shifts due to the non-polar environment around Trp assisted by polar charge-reinforced interactions.

After TL/CDs freeze-drying and reconstitution in PBS, the amount of TL in solution increased in a poorly predictable way. In fact, amorphous degree of the samples due to freeze-drying and establishment of novel TL/CDs interactions in an environment with different ionic strength and pH can concomitantly play a role, making dissection of the single contribution difficult to derive. Polymeric CDs were indeed found to be the most suitable derivative for TL solubilization while CMβCD was the best performer within the monomeric CD series (Fig. 5).

When considering potential applications of AMPs in therapy, skin and soft tissue infections, comprising those occurring in open wounds, are highly challenging since their treatment is complicate by the rise in multidrug resistant microorganisms and emergence of *MRSA* (Leong et al., 2018). As far as antimicrobial activity is concerned, all the data collected in our study point at TL as an efficient antimicrobial peptide against planktonic bacteria at very low concentrations (1–8 μM) and demonstrate that the association with CDs does not significantly influence these properties (Table 1).

Although acute infections are triggered by microbial cells that are in

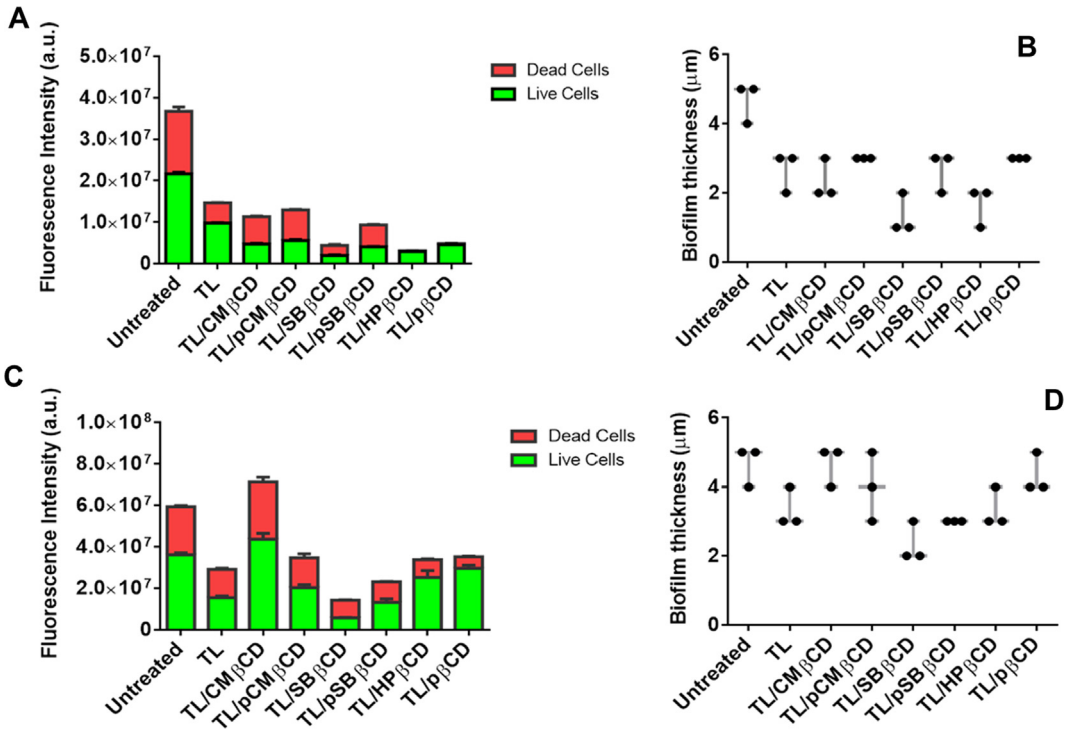

Fig. 9. Analysis of the effects of TL and TL/CDs on *MRSA* (A, B) and *P. aeruginosa* PAO1 (C, D) pre-formed biofilm. Fluorescence intensity (A, C) and biofilm thickness (B, D) were measured with using Zen Lite 2.3 software.

their planktonic forms, over time such microbes develop strategies to ensure their survival and adaptation to the stressful environments. This leads to the formation of a cohesive and strong community of cells that possess intercellular communication, known as biofilm (Zasloff, 2002). Indeed, biofilm infections are a key issue in chronic and long-term infections, including those colonizing medical devices and implants (Pletzer et al., 2016). Microorganisms growing in a biofilm state are very resilient to the treatment by many antimicrobial agents. Positively-charged molecules hardly cross biofilm due to electrostatic interactions with the extracellular matrix embedding bacteria, which is mainly made of anionic alginates. Consequently, drug ability to reach the target becomes poor and an increase of drug dose is the most common solution to adopt. Since interactions with CDs altered TL physical–chemical features, also TL transport rate in the biofilm could be altered.

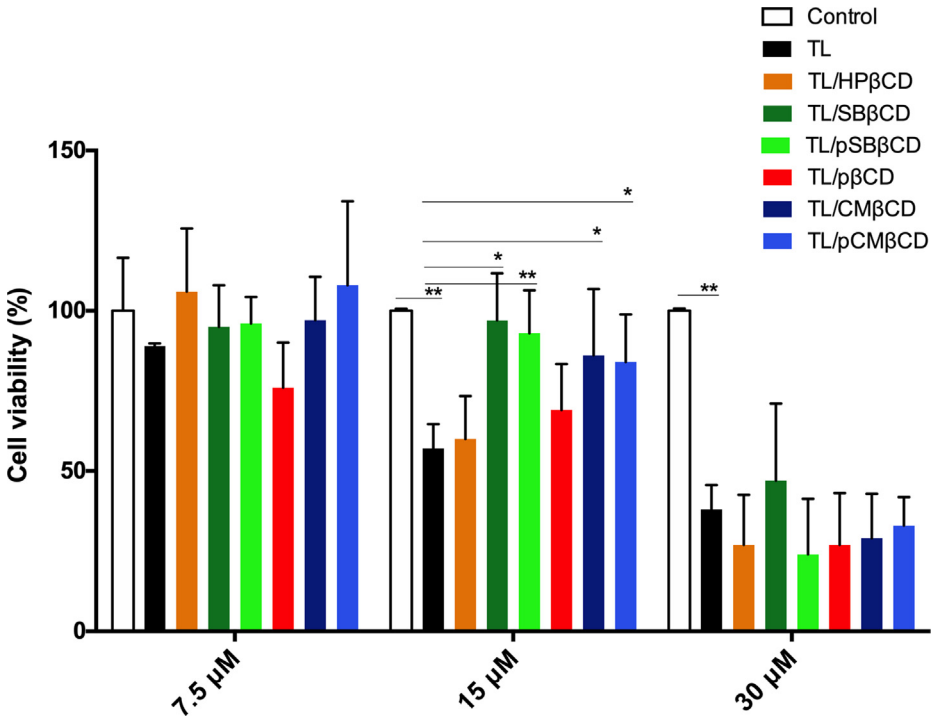

Fig. 10. MTT assay of different TL/βCD derivatives on HaCaT cell line. Cell viability is reported as percentage, compared to control (untreated cells). Three independent experiments were performed. *P < 0.05, **P < 0.01.

In order to evaluate this aspect in a simple and reproducible way, a transport experiment making use of bacterial alginates as a surrogate of extracellular matrix in the biofilm was performed. Interestingly, we found that pCMβCD ensured an increased rate of TL transport as a result of the effective shielding of TL interactions with alginates (Fig. 6). It is worth noting that the facilitated TL transport operated by neutral HPβCD can be attributed to its osmotic properties which promotes formation of a less tight alginate gel network.

Prompted by the ability of CDs to modulate TL transport throughout the alginates barrier, the anti-biofilm properties of TL and TL/CDs were investigated against clinical isolated of *P. aeruginosa* PAO1 and *MRSA* bacteria. We found that TL or TL/CDs are effective in hampering biofilm attachment, and, even more interestingly, they strongly affected pre-formed biofilms (Fig. 7B and D) even at TL concentration (0.25 μM) much lower than those required to directly kill planktonic cells. This is in agreement with previous reports indicating that several anti-microbial substances, such as the antimicrobial peptide LL-37, potently inhibits the formation of bacterial biofilms in vitro at a concentration significantly lower than that required to kill or inhibit bacterial growth (Overhage et al., 2008).

In the case of *MRSA,* we found that all TL/CDs were able to affect pre-formed biofilm, with the strongest effects observed in the case of TL/SBβCD and TL/HPβCD treatment (Figs. 8, 9A and B). For *P. aeruginosa* PAO1, similar results have been obtained, with the strongest effects again under TL/SBβCD treatment (Figs. 8, 9C and D). However, it should be noted that in the case of PAO1 the preformed biofilm treated with 0.25 μM TL/CMβCD gave no significant results (Fig. 8B) as in that biofilm height and fluorescence intensity appear similar to the control (Fig. 9C and D). On the other hand, when the treatment is carried out with the same TL in complex with pCMβCD, the biofilm eradication is significantly increased, indicating that the presence of strongly interacting CDs is decisive to penetrate PAO1 biofilm matrix. Altogether, these results indicate that most of the tested compounds significantly affect the biofilm attachment and eradication of both Gram-negative and Gram-positive bacterial strains, in agreement with the crystal violet data (Fig. 7). Based on our observations, it is possible to hypothesize that TL/CDs exert their effects through different mechanisms of action on Gram-positive and Gram-negative bacteria. The overall data allow to speculate that successful therapeutic approaches could be designed by combining TL with selected CDs on bacterial cells entrapped into the biofilm structure.

Finally, the cytotoxicity assay on human keratinocytes (HaCaT cells, Fig. 10) showed that 15 μM of TL/SBβCD, TL/pSBβCD, TL/CMβCD and TL/pCMβCD complexes have highly reduced toxic effect compared to TL alone, indicating a protective effect of these CDs on HaCaT cells against TL toxicity. The effect can be tentatively rationalized considering that TL interacts with eukaryotic cells by deeply inserting its N-terminal region into the cell membrane (Saviello et al., 2010). CDs bound to TL can partially hide this peptide region (Fig. 4) thus making more difficult TL membrane perturbation. Notably, TL/SBβCD, TL/pSBβCD, TL/CMβCD and TL/pCMβCD are the most stable complexes having the greatest hypsochromic shift in their fluorescence emission spectra (Figs. 2 and 5) and the greatest signal shifts in the NMR spectra (Fig. 4 and S8). TL/HPβCD and TL/pβCD associate through weak interaction and therefore it is expected that free TL is mainly acting.

5. Conclusion

Main results indicate that association of TL with selected CDs can be safer than TL alone while maintaining antibacterial activity against planktonic bacteria. Interestingly, CDs can modulate TL ability to cross alginates barriers which parallels complexes capabilities in inhibition/reduction of biofilm in both Gram-positive and Gram-negative bacterial strains. Overall, the results ascertained the possibility that TL/CDs complexes can be considered as future antimicrobial weapons especially against biofilm-producing bacteria. Our result can be considered a more general proof of concept demonstrating the suitability of complexes of CDs with many other cationic AMPs in order to optimize AMPs as antimicrobial agents.

CRediT authorship contribution statement

Diego Brancaccio: Investigation, Visualization, Validation, Data curation. **Elio Pizzo:** Investigation, Visualization, Validation, Writing - original draft, Writing - review & editing. **Valeria Cafaro:** Investigation, Visualization, Validation, Funding acquisition. **Eugenio Notomista:** Investigation, Visualization, Validation, Writing - original draft, Writing - review & editing. **Federica De Lise:** Investigation, Visualization, Validation, Data curation. **Andrea Bosso:** Investigation, Visualization, Validation, Data curation. **Rosa Gaglione:** Investigation, Visualization, Validation, Data curation. **Francesco Merlino:** Investigation, Visualization, Validation, Data curation. **Ettore Novellino:** Investigation, Writing - original draft, Writing - review & editing. **Francesca Ungaro:** Investigation, Visualization, Validation, Data curation. **Paolo Grieco:** Investigation, Visualization, Validation, Writing - original draft, Writing - review & editing. **Milo Malanga:** Investigation, Visualization, Validation, Data curation. **Fabiana Quaglia:** Conceptualization, Writing original-draft, Writing - review & editing. **Agnese Miro:** Investigation, Funding acquisition,. **Alfonso Carotenuto:** Conceptualization, Supervision, Funding acquisition, Writing original-draft, Writing - review & editing.

Declaration of Competing Interest

The authors declare that they have no known competing financial interests or personal relationships that could have appeared to influence the work reported in this paper.

Acknowledgments

This research was financially supported by the University of Naples “Federico II”: Finanziamento della ricerca di Ateneo - Università degli Studi di Napoli Federico II - Annualità 2016; prot. number 16503.

Appendix A. Supplementary data

Supplementary data to this article can be found online at https://doi.org/10.1016/j.ijpharm.2020.119437.

References

Antunes, D.A., Moll, M., Devaurs, D., Jackson, K.R., Lizée, G., Kavraki, L.E., 2017. DINC 2.0: A new protein-peptide docking webserver using an incremental approach. Cancer Res. 77, 55–57. https://doi.org/10.1158/0008-5472.CAN-17-0511.

Bosso, A., Pirone, L., Gaglione, R., Pane, K., Del Gatto, A., Zaccaro, L., Di Gaetano, S., Diana, D., Fattorusso, R., Pedone, E., Cafaro, V., Haagsman, H.P., van Dijk, A., Scheenstra, M.R., Zanfardino, A., Crescenzi, O., Arciello, A., Varcamonti, M., Veldhuizen, E.J.A., Di Donato, A., Notomista, E., Pizzo, E., 2017. A new cryptic host defense peptide identified in human 11-hydroxysteroid dehydrogenase-1 β-like: from in silico identification to experimental evidence. Biochim. Biophys. Acta - Gen. Subj. 1861, 2342–2353. https://doi.org/10.1016/j.bbagen.2017.04.009.

Braunschweiler, L., Ernst, R.R., 1983. Coherence transfer by isotropic mixing: Application to proton correlation spectroscopy. J. Magn. Reson. 53, 521–528. https://doi.org/10.1016/0022-2364(83)90226-3.

Brogden, K.A., 2005. Antimicrobial peptides: pore formers or metabolic inhibitors in bacteria? Nat. Rev. Microbiol. 3, 238–250. https://doi.org/10.1038/nrmicro1098.

Buommino, E., Carotenuto, A., Antignano, I., Bellavita, R., Casciaro, B., Loffredo, M.R., Merlino, F., Novellino, E., Mangoni, M.L., Nocera, F.P., Brancaccio, D., Punzi, P., Roversi, D., Ingenito, R., Bianchi, E., Grieco, P., 2019. The Outcomes of Decorated Prolines in the Discovery of Antimicrobial Peptides from Temporin-L. ChemMedChem 14, 1283–1290. https://doi.org/10.1002/cmdc.201900221.

Carotenuto, A., Malfi, S., Saviello, M.R., Campiglia, P., Gomez-Monterrey, I., Mangoni, M.L., Gaddi, L.M.H., Novellino, E., Grieco, P., 2008. A different molecular mechanism underlying antimicrobial and hemolytic actions of temporins A and L. J. Med. Chem. 51, 2354–2362. https://doi.org/10.1021/jm701604t.

Challa, R., Ahuja, A., Ali, J., Khar, R.K., 2005. Cyclodextrins in drug delivery: An updated review. AAPS PharmSciTech 6, 329–357. https://doi.org/10.1208/pt060243.

Cornick, S., Tawiah, A., Chadee, K., 2015. Roles and regulation of the mucus barrier in the gut. Tissue Barriers 1–2. https://doi.org/10.4161/21688370.2014.982426.
D'Angelo, I., Casciaro, B., Miro, A., Quaglia, F., Mangoni, M.L., Ungaro, F., 2015. Overcoming barriers in Pseudomonas aeruginosa lung infections: Engineered nanoparticles for local delivery of a cationic antimicrobial peptide. Colloids Surfaces B Biointerfaces 135, 717–725. https://doi.org/10.1016/j.colsurfb.2015.08.027.
Dhanik, A., McMurray, J.S., Kavraki, L.E., 2013. DINC: A new AutoDock-based protocol for docking large ligands. BMC Struct. Biol. 13, S1–S11. https://doi.org/10.1186/1472-6807-13-S1-S11.
Gaglione, R., Dell'Olmo, E., Bosso, A., Chino, M., Pane, K., Ascione, F., Itri, F., Caserta, S., Amoresano, A., Lombardi, A., Haagsman, H.P., Piccoli, R., Pizzo, E., Veldhuizen, E.J.A., Notomista, E., Arciello, A., 2017. Novel human bioactive peptides identified in Apolipoprotein B: Evaluation of their therapeutic potential. Biochem. Pharmacol. 130, 34–50. https://doi.org/10.1016/j.bcp.2017.01.009.
Grieco, P., Carotenuto, A., Auriemma, L., Saviello, M.R., Campiglia, P., Gomez-Monterrey, I.M., Marcellini, L., Luca, V., Barra, D., Novellino, E., Mangoni, M.L., 2013. The effect of d-amino acid substitution on the selectivity of temporin L towards target cells: Identification of a potent anti-Candida peptide. Biochim. Biophys. Acta - Biomembr. https://doi.org/10.1016/j.bbamem.2012.08.027.
Grieco, P., Luca, V., Auriemma, L., Carotenuto, A., Saviello, M.R., Campiglia, P., Barra, D., Novellino, E., Mangoni, M.L., 2011. Alanine scanning analysis and structure-function relationships of the frog-skin antimicrobial peptide temporin-1Ta. J. Pept. Sci. https://doi.org/10.1002/psc.1350.
Hwang, T.L., Shaka, A.J., 1995. Water Suppression That Works. Excitation Sculpting Using Arbitrary Wave-Forms and Pulsed-Field Gradients. J. Magn. Reson. Ser. A 112, 275–279. https://doi.org/10.1006/jmra.1995.1047.
Jacob, J.T., Klein, E., Laxminarayan, R., Beldavs, Z., Lynfield, R., Kallen, A.J., Ricks, P., Edwards, J., Srinivasan, A., Fridkin, S., Rasheed, K.J., Lonsway, D., Bulens, S., Herrera, R., McDonald, C.L., Patel, J., Limbago, B., Bell, M., Cardo, D., 2013. Vital signs: Carbapenem-resistant enterobacteriaceae. Morb. Mortal. Wkly. Rep. 62, 165–170.
Jeener, J., Meier, B.H., Bachmann, P., Ernst, R.R., 1979. Investigation of exchange processes by two-dimensional NMR spectroscopy. J. Chem. Phys. 71, 4546. https://doi.org/10.1063/1.438208.
Leong, H.N., Kurup, A., Tan, M.Y., Kwa, A.L.H., Liau, K.H., Wilcox, M.H., 2018. Management of complicated skin and soft tissue infections with a special focus on the role of newer antibiotics. Infect. Drug Resist. 1959–1974. https://doi.org/10.2147/IDR.S172366.
Mahalka, A.K., Kinnunen, P.K.J., 2009. Binding of amphipathic α-helical antimicrobial peptides to lipid membranes: Lessons from temporins B and L. Biochim. Biophys. Acta - Biomembr. 1600–1609. https://doi.org/10.1016/j.bbamem.2009.04.012.
Malanga, M., Bálint, M., Puskás, I., Tuza, K., Sohajda, T., Jicsinszky, L., Szente, L., Fenyvesi, É., 2014. Synthetic strategies for the fluorescent labeling of epichlorohydrin-branched cyclodextrin polymers. Beilstein J. Org. Chem. 10, 3007–3018. https://doi.org/10.3762/bjoc.10.319.
Merlino, F., Carotenuto, A., Casciaro, B., Martora, F., Loffredo, M.R., Di Grazia, A., Yousif, A.M., Brancaccio, D., Palomba, L., Novellino, E., Galdiero, M., Iovene, M.R., Mangoni, M.L., Grieco, P., 2017. Glycine-replaced derivatives of [Pro3, DLeu9]TL, a temporin L analogue: Evaluation of antimicrobial, cytotoxic and hemolytic activities. Eur. J. Med. Chem. 139, 750–761. https://doi.org/10.1016/j.ejmech.2017.08.040.
Merlino, F., Tomassi, S., Yousif, A.M., Messere, A., Marinelli, L., Grieco, P., Novellino, E., Cosconati, S., Di Maro, S., 2019. Boosting Fmoc Solid-Phase Peptide Synthesis by Ultrasonication. Org. Lett. 21, 6378–6382. https://doi.org/10.1021/acs.orglett.9b02283.
Miro, A., Ungaro, F., Quaglia, F., 2011. Cyclodextrins as Smart Excipients in Polymeric Drug Delivery Systems. In: Bilensoy, E. (Ed.), Cyclodextrins in Pharmaceutics, Cosmetics, and Biomedicine: Current and Future Industrial Applications. John Wiley and Sons, USA, pp. 65–89. https://doi.org/10.1002/9780470926819.
Mookherjee, N., Hancock, R.E.W., 2007. Cationic host defence peptides: Innate immune regulatory peptides as a novel approach for treating infections. Cell. Mol. Life Sci. 922–933. https://doi.org/10.1007/s00018-007-6475-6.
Overhage, J., Campisano, A., Bains, M., Torfs, E.C.W., Rehm, B.H.A., Hancock, R.E.W., 2008. Human host defense peptide LL-37 prevents bacterial biofilm formation. Infect. Immun. 76, 4176–4182. https://doi.org/10.1128/IAI.00318-08.
Pandey, S., Kumar, B., Swamy, S.M.V., Gupta, A., 2010. A review on pharmaceutical application of cyclodextrins. Sect. Title Pharm. 2, 281–319.
Pletzer, D., Coleman, S.R., Hancock, R.E.W., 2016. Anti-biofilm peptides as a new weapon in antimicrobial warfare. Curr. Opin. Microbiol. 35–40. https://doi.org/10.1016/j.mib.2016.05.016.
Rinaldi, A.C., Mangoni, M.L., Rufo, A., Luzi, C., Barra, D., Zhao, H., Kinnunen, P.K.J., Bozzi, A., Di Giulio, A., Simmaco, M., 2002. Temporin L: Antimicrobial, haemolytic and cytotoxic activities, and effects on membrane permeabilization in lipid vesicles. Biochem. J. 368, 91–100. https://doi.org/10.1042/BJ20020806.
Römling, U., Balsalobre, C., 2012. Biofilm infections, their resilience to therapy and innovative treatment strategies. J. Intern. Med. https://doi.org/10.1111/joim.12004.
Saviello, M.R., Malfi, S., Campiglia, P., Cavalli, A., Grieco, P., Novellino, E., Carotenuto, A., 2010. New insight into the mechanism of action of the temporin antimicrobial peptides. Biochemistry. https://doi.org/10.1021/bi902166d.
Simmaco, M., Mignogna, G., Canofeni, S., Miele, R., Mangoni, M.L., Barra, D., 1996. Temporins, antimicrobial peptides from the European red frog Rana temporaria. Eur. J. Biochem. 242, 788–792. https://doi.org/10.1111/j.1432-1033.1996.0788r.x.
States, D.J., Haberkorn, R.A., Ruben, D.J., 1982. A two-dimensional nuclear overhauser experiment with pure absorption phase in four quadrants. J. Magn. Reson. 48, 286–292. https://doi.org/10.1016/0022-2364(82)90279-7.
Teale, F.W., 1960. The ultraviolet fluorescence of proteins in neutral solution. Biochem. J. 72, 381–388. https://doi.org/10.1042/bj0760381.
Uekama, K., Hirayama, F., Arima, H., 2006. Recent aspect of cyclodextrin-based drug delivery system. J. Incl. Phenom. Macrocycl. Chem. 3–8. https://doi.org/10.1007/s10847-006-9052-y.
Wiegand, I., Hilpert, K., Hancock, R.E.W., 2008. Agar and broth dilution methods to determine the minimal inhibitory concentration (MIC) of antimicrobial substances. Nat. Protoc. 3, 163–175. https://doi.org/10.1038/nprot.2007.521.
Woodford, N., Wareham, D.W., Guerra, B., Teale, C., 2014. Carbapenemase-producing enterobacteriaceae and non-enterobacteriaceae from animals and the environment: An emerging public health risk of our own making? J. Antimicrob. Chemother. 69, 287–291. https://doi.org/10.1093/jac/dkt392.
Wüthrich, K., 1986. NMR of Proteins and Nucleic Acids. New York. https://doi.org/10.1039/b618334b.
Yeguas, V., Altarsha, M., Monard, G., López, R., Ruiz-López, M.F., 2011. Peptide binding to β-cyclodextrins: Structure, dynamics, energetics, and electronic effects. J. Phys. Chem. A 115, 11810–11817. https://doi.org/10.1021/jp2053037.
Zasloff, M., 2002. Antimicrobial peptides of multicellular organisms. Nature 389–395. https://doi.org/10.1038/415389a.